Scientific Research Publishing

Journal of Applied Mathematics and Physics, 2024, 12, 3017-3025
https://www.scirp.org/journal/jamp
ISSN Online: 2327-4379
ISSN Print: 2327-4352

Analyzing Thermal Stratification and Nanoparticle Shapes Influence on an EMHD Ternary Nanofluid Flow amidst Two Spinning Disks

Muhammad Ramzan[1*], Saima Riasat[2]

[1]Department of Computer Science, Bahria University, Islamabad, Pakistan
[2]Department of Mathematical Science, Fatima Jinnah Women University, Rawalpindi, Pakistan
Email: *mramzan@bahria.edu.pk

How to cite this paper: Ramzan, M. and Riasat, S. (2024) Analyzing Thermal Stratification and Nanoparticle Shapes Influence on an EMHD Ternary Nanofluid Flow amidst Two Spinning Disks. *Journal of Applied Mathematics and Physics*, **12**, 3017-3025.
https://doi.org/10.4236/jamp.2024.128180

Received: July 8, 2024
Accepted: August 27, 2024
Published: August 30, 2024

Abstract

The present study examines the thermal distribution of ternary nanofluid flow amid two spinning disks influenced by electric and magnetic fields. Keeping in view the shape of the particles, the electrically conducting ternary nanofluid is analyzed with variable thermophysical features. Three types of nanoparticles namely Copper, Aluminum Oxide, and Graphene with spherical, cylindrical, and platelet shapes are taken respectively and are immersed in a (50-50)% ratio of water and ethylene glycol mixture which acts as a base fluid. The anticipated problem is addressed by employing a reliable and user-friendly numerical bvp4c built-in collocation scheme. This solution is then showcased through illustrations and tables. Strengthening the radiation results in an enhanced heat transfer rate. Radial and azimuthal velocities once rotation of disks is enhanced. The key findings provide a strong theoretical background in photovoltaic cells, solar collectors, radiators, solar water heaters, and many other applications.

Keywords

Trihybrid Nanofluid Flow, Thermal Stratification, Particle Shapes, Spinning Disks

1. Introduction

Nanofluids have promising thermophysical features to improve heat transfer rates. Their superior thermal conductivity compared to regular fluids motivated

researchers to explore a wider range of nanofluids. Nanofluids are commonly a mixture of nanoparticles and a customary liquid. Nanoparticles may be from metals, oxides, carbides, and carbon nanotubes family, and alcohol, ethylene glycol, water, oil., etc. are mostly used as base liquids. Choi [1] first anticipated the idea to study the nanofluids. Masuda *et al.* [2] focused on the dispersion of nanoparticles to alter the thermal conductivity and viscosity of nanofluid. Metallic and nonmetallic oxides, Nitrides, and carbides suspended in base fluid are studied experimentally and theoretically by various researchers [3]-[7]. With the improved thermal stability, thermal conductivity, and thermal properties a new kind of nanofluid known as hybrid nanofluid is recently introduced. Two or more kinds of nanoparticles are employed in a customary fluid to synthesize the hybrid nanofluid. Numerical and experimental research on hybrid nanofluid flows is available in the literature. Huminic and Huminic [8] have scrutinized the applications of hybrid nanofluids in varied scenarios. It is observed that convective heat transfer in heat exchangers can be improved by increasing pressure drop and pumping power of fluid. Hussein *et al.* [9] emphasized the heat transfer improvement of silica and titanium dioxide in automotive cooling systems. Various researchers [10] [11] employed various kinds of nanoparticles to study the enhanced thermophysical features of a hybrid nanofluid.

Nanoparticle response to electric and magnetic fields is an interesting phenomenon to enhance the heat transfer rate. Electromagnetohydrodynamic (EMHD) is a technique that significantly augments the heat transfer rate in the hybrid and nanofluid flows. It has found tremendous applications in fusion reactions, magnetospheres, plasma confinement, cosmic plasma, biomedical engineering, and various practical implementations. Swallom *et al.* [12] studied the submarine propulsion application of magnetohydrodynamics. In this analysis, various configurations and geometries have been analyzed. Chen *et al.* [13] deliberated a statistical structure analysis of an MHD thruster in a helical channel. Khan and Kosel [14] utilized the laser-induced graphene electrodes with an MHD pump with polydimethylsiloxane as a substrate. Waqas *et al.* [15] studied the EMHD effects on the heat transfer improvement of hybrid nanofluid flow between two rotating plates. Haq *et al.* [16] dedicated to elaborating the heat transfer enhancement of nanofluid with carbon nanotubes as nanoparticles under MHD effects between two rotating disks.

After a brief literature review, it has been inferred that various studies have incorporated the hybrid nanofluid flow amid two rotating disks. However, incorporating three kinds of nanocomposites by considering the shape of particles in the presence of electric and magnetic fields is the novelty of the problem. The collocation method is applied to solve the highly nonlinear problem. The outcomes are presented both graphically and in tabular format.

2. Mathematical Model

Consider ternary nanofluid with Spherical Cu, cylindrical Al_2O_3 and platelet graphene particles with 50% water and 50% ethylene glycol as a base fluid amid two

rotating electrodes with angular velocity in the shape of disks. The magnetic field of strength $\boldsymbol{B} = B_o$ applied in the normal direction accompanying a uniform electric field $\boldsymbol{E} = \tilde{E}_o = E_o r\omega$ are engaged. It is assumed that flow is between the disks placed at $Z = 0$ and $Z = d$. The description of the flow geometry is given in **Figure 1**.

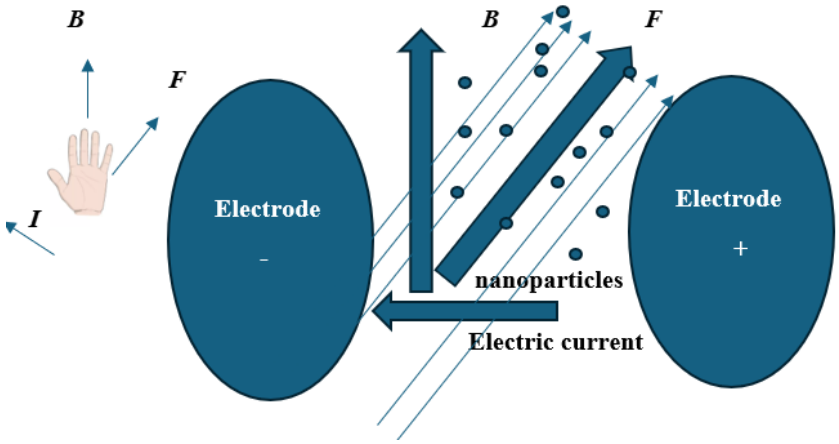

Figure 1. Geometrical Configuration of model.

Considering the above assumption the mathematical model takes the following form:

$$u_r + \frac{u}{r} + w_z = 0, \tag{1}$$

$$u_t + uu_r + wu_z - \frac{\upsilon^2}{r} = -\frac{1}{\rho_{tnf}}\frac{\partial p}{\partial r} + \frac{\mu_{tnf}}{\rho_{tnf}}\left(u_{rr} + \frac{1}{r}u_r - \frac{u}{r^2} + u_{zz}\right) + \frac{\sigma_{tnf}}{\rho_{tnf}}\left(EB_o - B_o^2 u\right), \tag{2}$$

$$v_t + uv_r + wv_z + \frac{uv}{r} = \frac{\mu_{tnf}}{\rho_{tnf}}\left(v_{rr} + \frac{1}{r}v_r - \frac{v}{r^2} + v_{zz}\right) + \frac{\sigma_{tnf}}{\rho_{tnf}}\left(EB_o - B_o^2 v\right), \tag{3}$$

$$w_t + uw_r + ww_z - \frac{v^2}{r} = -\frac{1}{\rho_{tnf}}\frac{\partial p}{\partial z} + \frac{\mu_{tnf}}{\rho_{tnf}}\left(w_{rr} + \frac{1}{r}w_r + w_{zz}\right), \tag{4}$$

$$uT_r + wT_z = \frac{K_{tnf}}{(\rho C_p)_{tnf}}\left(T_{rr} + \frac{1}{r}T_r + T_{zz}\right) + \frac{16\sigma^* T_L^3}{3k^*(\rho C_p)_{nf}}T_{zz} + \frac{\sigma_{tnf}}{(\rho C_p)_{tnf}}\left(E_o - B_o(u+v)^2\right). \tag{5}$$

Thermal stratification at the lower and the upper disks are $T_1 = T_0 + A'r/1-ct$, and $T_2 = T_0 + B'r/1-ct$ respectively. The boundary constraints are:

$$u = \frac{ra_1}{1-ct}, v = \frac{r\Omega_1}{1-ct}, w = 0, T = T_1 = T_0 + \frac{A'r}{1-ct}, z = 0, \tag{6}$$

$$u = \frac{ra_2}{1-ct}, v = \frac{r\Omega_2}{1-ct}, w = 0, T = T_2 = T_0 + \frac{B'r}{1-ct}, z = h. \tag{7}$$

Here k^* and σ^* denote the coefficient of mean absorption and Stefan Boltzmann constant respectively. By introducing three nanoparticles of spherical cylindrical and platelet shape, thermophysical properties are described as under:

$$k_{tnf} = \left(k_{nf1}\varphi_3 + k_{nf2}\varphi_1 + k_{nf3}\varphi_2\right)\varphi^{-1} \tag{8}$$

$$\mu_{tnf} = \left(\mu_{nf1}\varphi_3 + \mu_{nf2}\varphi_1 + \mu_{nf3}\varphi_2\right)\varphi^{-1} \tag{9}$$

To define the shape of nanoparticles in spherical form we write:

$$\mu_{tnf1} = \left(6.2\varphi^2 + 2.5\varphi + 1\right)\mu_{bf}, \tag{10}$$

$$k_{nf1} = \left(\frac{-2\varphi(k_{bf} - k_{sp1}) + 2k_{bf} + k_{sp1}}{\varphi(k_{bf} - k_{sp1}) + 2k_{bf} + k_{sp1}}\right)k_{bf}, \tag{11}$$

For cylindrical-shaped nanoparticle:

$$\mu_{tnf2} = \left(904.4\varphi^2 + 13.5\varphi + 1\right)\mu_{bf}, \tag{12}$$

$$k_{nf2} = \left(\frac{-3.9\varphi(k_{bf} - k_{sp2}) + 3.9k_{bf} + k_{sp2}}{\varphi(k_{bf} - k_{sp2}) + 2k_{bf} + k_{sp2}}\right)k_{bf}, \tag{13}$$

and for platelet-shaped nanoparticles, we have:

$$\mu_{tnf3} = \left(612.6\varphi^2 + 37.1\varphi + 1\right)\mu_{bf}, \tag{14}$$

$$k_{nf3} = \left(\frac{-4.7\varphi(k_{bf} - k_{sp3}) + 4.7k_{bf} + k_{sp3}}{\varphi(k_{bf} - k_{sp3}) + 2k_{bf} + k_{sp3}}\right)k_{bf}. \tag{15}$$

The mathematical model for viscosity density, specific heat, and thermal conductivity is as follows:

$$\rho_{tnf} = \left(1 - \varphi_1 - \varphi_2 - \varphi_3\right)\rho_{bf} + \varphi_3\rho_{sp3} + \varphi_2\rho_{sp2} + \varphi_1\rho_{sp1}, \tag{16}$$

$$\begin{aligned}\left(\rho C_p\right)_{tnf} &= \left(1 - \varphi_1 - \varphi_2 - \varphi_3\right)\left(\rho C_p\right)_{bf} + \\ &\varphi_3\left(\rho C_p\right)_{sp3} + \varphi_2\left(\rho C_p\right)_{sp2} + \varphi_1\left(\rho C_p\right)_{sp1},\end{aligned} \tag{17}$$

$$k_{tnf} = \left(\varphi_1 k_{sp1} + \varphi_2 k_{sp2} + \varphi_3 k_{sp3}\right)/\left(\varphi_1 + \varphi_2 + \varphi_3\right) \tag{18}$$

where $\varphi = \varphi_1 + \varphi_2 + \varphi_3$.

Table 1 represents the thermo-physical characteristics of spherically shaped Cu, with cylindrical orientation Al_2O_3, and platelet-shaped graphene.

Table 1. Thermo-physical properties of Ethylene Glycol and nanoparticles.

Physical Properties	Cu Spherical	Al_2O_3 Cylindrical	Graphene Platelet	50% Ethylene Glycol and 50% Water
$\rho(\frac{\text{kg}}{\text{m}^3})$	8954	3970	2200	1056
$C_p(\frac{\text{JK}}{\text{kg}})$	383	765	790	3288
$k(\frac{\text{W}}{\text{mK}})$	400	40	5000	0.425

The following transformation converts the above nonlinear set of Equations (2)-(7) to the ensuing dimensionless form:

$$\begin{aligned} u &= \frac{r\Omega_1}{1-ct} f'(\eta), v = \frac{r\Omega_1}{1-ct} g(\eta), \\ w &= \frac{2h\Omega_1}{\sqrt{1-ct}} f(\eta), \theta = \frac{T-T_2}{T_1-T_o}, \eta = \frac{z}{h\sqrt{1-ct}}. \end{aligned} \tag{19}$$

The non-dimensional form is:

$$f''' + \mathrm{Re}\left(\left(f'^2 - 2ff'' - g^2 \right) - \frac{1}{2} A_1 \zeta \frac{B_2}{B_1} f'' - \frac{M}{B_1} \left(f' + E_1 \right) - A_1 f' \right) = 0, \tag{20}$$

$$\left[2\left(f'g - fg' \right) + \frac{A_1}{2} \zeta g' + A_1 g + M\left(E_1 - g \right) \right] = \frac{B_1}{B_2 \,\mathrm{Re}} g'', \tag{21}$$

$$\frac{1}{\mathrm{Pr}\,\mathrm{Re}} \frac{B_4}{B_3} \theta''(1+R) + 2f\theta' - \frac{\zeta A_1}{2} \theta' + MEc\left(E_1 - (f'+g)^2 \right) = 0. \tag{22}$$

The boundary constraints are transformed into:

$$\begin{aligned} &f(0) = 0,\ f(1) = 0,\ f'(0) = \gamma_1,\ f'(1) = \gamma_2, \\ &g(0) = 1,\ g(1) = \Omega,\ \theta(0) = 1-s,\ \theta(1) = 0, \end{aligned} \tag{23}$$

where

$$\begin{aligned} &M = \frac{\sigma_f B_o^2 (1-ct)}{\rho_f \left(1+m^2\right)},\ A_1 = \frac{c}{\Omega_1},\ \gamma_1 = \frac{a_1}{\Omega_1},\ \gamma_2 = \frac{a_2}{\Omega_2},\ \Omega = \frac{\Omega_2}{\Omega_1}, \\ &R = \frac{-16\sigma^* T_L^3}{3k_f k^*},\ Pr = \frac{\upsilon_f \left(\rho C_p\right)_f}{k_f},\ B_1 = \frac{\rho_{tnf}}{\rho_f},\ B_2 = \frac{\mu_{tnf}}{\mu_f}, \\ &B_3 = \frac{\left(\rho C_p\right)_{tnf}}{\left(\rho C_p\right)_f},\ B_4 = \frac{k_{tnf}}{k_f}. \end{aligned} \tag{24}$$

Here, M is the magnetic moment parameter, A_1 is the parameter of unsteadiness, γ_1 and γ_2 are the parameters of scale stretching, Ω is the parameter of rotation, R is the radiation parameter, Pr is the Prandtl number, B_1, B_2, B_3 and B_4 are used to denote the thermophysical properties of nanoparticles.

3. Results and Discussion

This section serves to display the outcomes in the form of illustrations and tables. **Figure 2** is the graphical outcome of the radial velocity profile for the magnetic field parameter. As the magnetic field strength parameter elevates it boosts resistance in fluid and surface. Resultantly the deceleration in flow velocity occurs near the surface of the lower disk. However, near the upper disk opposite trend in fluid motion is witnessed. The trend in the radial velocity profile for increasing values of Reynolds number Re is displayed in **Figure 3**. Near the lower disk, the deceleration in fluid motion is observed due to the radial flux of the lower disk. Additionally, an upsurge in Reynolds number causes the enhancement in inertial forces which slow down the flow phenomenon near the lower disk. However, as

the axial motion arises due to the vertical motion of the upper disk, radial velocity is seen to be increasing.

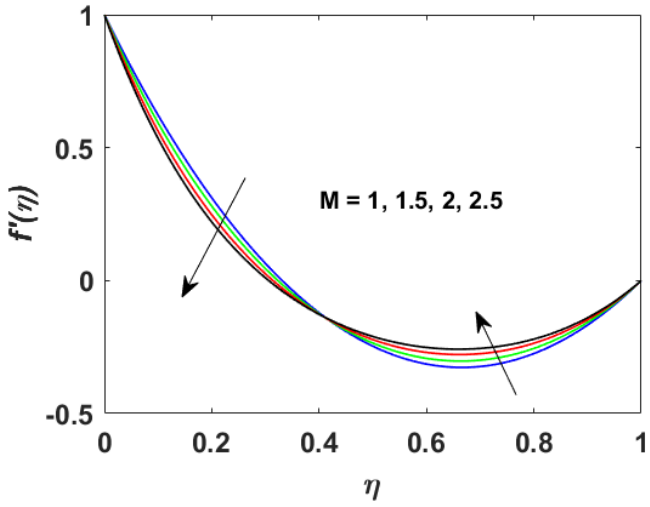

Figure 2. Radial velocity profile versus Magnetization parameter *M*.

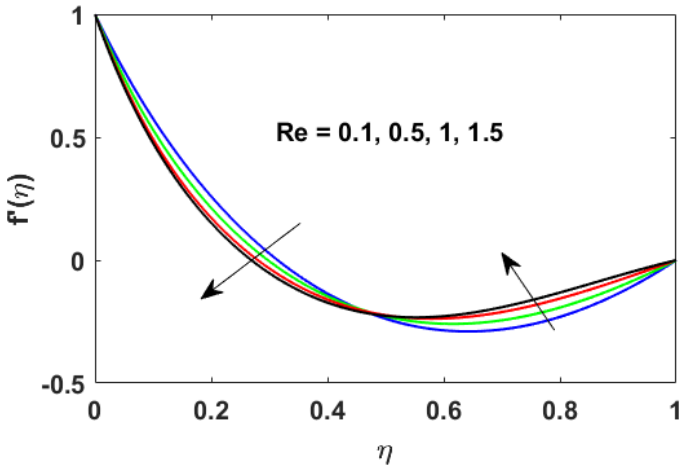

Figure 3. Radial velocity profile versus Reynolds number Re.

Figure 4 is the manifestation of the axial velocity profile for growing values of rotation parameter. For the growing values of the rotation parameter, the deceleration of the fluid motion near the lower while the acceleration near the upper disk is observed. This is because the rotation of the disks opposes the flow direction in the vicinity of both disks. Therefore, the opposite trend is observed in fluid motion for both disks for increasing rotation. The temperature profile for increasing values of thermal stratification parameter for rotating disks is given in **Figure 5**.

It is gained that increasing values of the thermal stratification parameter causes the cooling of disks. The physical significance behind the noted phenomenon is that the heat transfer rate is enhanced, and the thermal boundary layers' thickness gets thinner.

Figure 6 shows the temperature distribution for increasing values of radiation

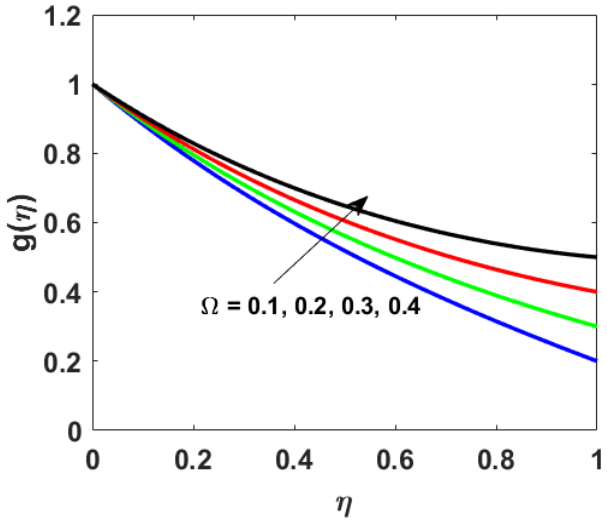

Figure 4. Axial velocity profile versus Rotation parameter Ω.

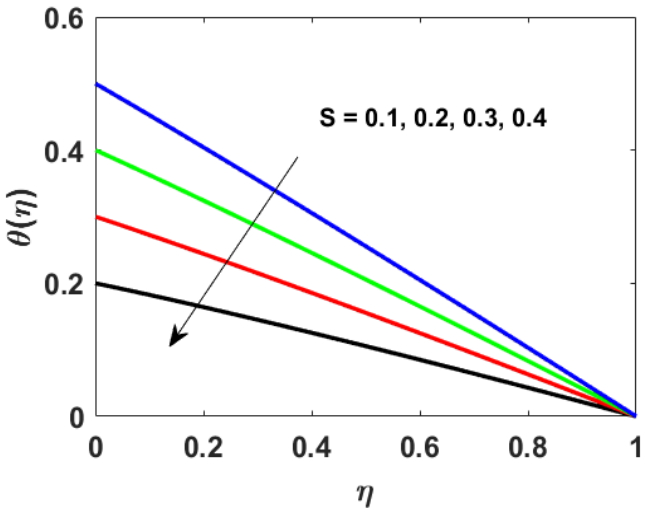

Figure 5. Temperature profile versus Rotation parameter Ω.

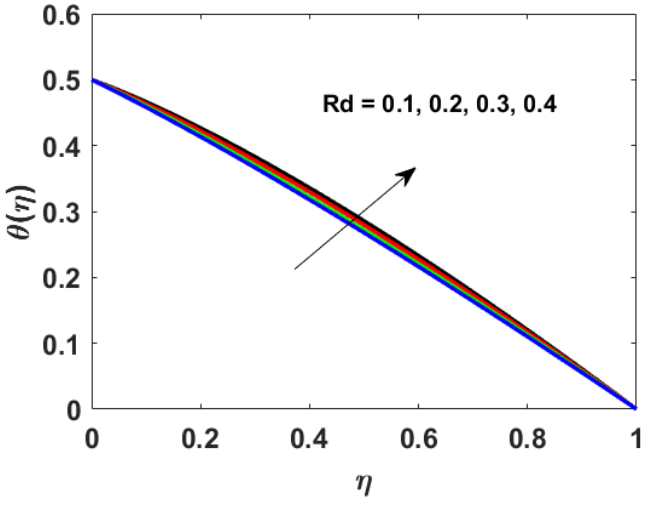

Figure 6. Temperature profile versus Radiation parameter *Rd*.

parameters. It is noted that as the values of radiation parameter increase both disks are heated. Increasing values of radiation parameter decay the mean absorption coefficient thereby, the temperature rises.

4. Conclusions

The present study has focused on ternary nanofluid flow by incorporating varied nanoparticles with dissimilar shapes. The said trihybrid nanofluid has a combination of three nanoparticles (copper, aluminum oxide, and graphene) and a base fluid (mixture of water and ethylene glycol with equal distribution). Three dissimilar shapes spherical, cylindrical, and platelet of copper, aluminum oxide, and graphene are considered respectively. The flow is assumed between two spinning disks under the influence of electric and magnetic fields. The graphical and numerical outcomes ascertain the following outcomes:

- Magnetic field strength causes the enhancement in radial and azimuthal velocity profiles due to the increasing strength of the Lorentz force.
- Owing to enhancement in the rotation characteristics of the plates, deceleration in the fluid motion is witnessed but a pronounced increment in the temperature profile.
- The increasing values of the rotation parameter enhance the inertial forces and therefore upsurge in radial and azimuthal velocity profiles is observed.
- The heat transfer rate can be boosted by intensifying the radiation parameter.

Conflicts of Interest

The authors declare no conflicts of interest regarding the publication of this paper.

References

[1] Choi, S.U. and Eastman, J.A. (1995) Enhancing Thermal Conductivity of Fluids with Nanoparticles. Argonne National Laboratory (ANL).

[2] Masuda, H., Ebata, A., Teramae, K. and Hishinuma, N. (1993) Alteration of Thermal Conductivity and Viscosity of Liquid by Dispersing Ultra-Fine Particles. Dispersion of Al_2O_3, SiO_2 and TiO_2 Ultra-Fine Particles. *Netsu Bussei*, **7**, 227-233. https://doi.org/10.2963/jjtp.7.227

[3] Akilu, S., Sharma, K.V., Baheta, A.T. and Mamat, R. (2016) A Review of Thermophysical Properties of Water Based Composite Nanofluids. *Renewable and Sustainable Energy Reviews*, **66**, 654-678.https://doi.org/10.1016/j.rser.2016.08.036

[4] Bakthavatchalam, B., Habib, K., Saidur, R., Saha, B.B. and Irshad, K. (2020) Comprehensive Study on Nanofluid and Ionanofluid for Heat Transfer Enhancement: A Review on Current and Future Perspective. *Journal of Molecular Liquids*, **305**, Article ID: 112787. https://doi.org/10.1016/j.molliq.2020.112787

[5] Buongiorno, J. and Hu, L.W. (2009) Nanofluid Heat Transfer Enhancement for Nuclear Reactor Applications. *ASME* 2009 *Second International Conference on Micro/Nanoscale Heat and Mass Transfer*, 18-21 December 2009, Shanghai, 517-522. https://doi.org/10.1115/MNHMT2009-18062

[6] Sheikholeslami, M.M.S.N., Rezaeianjouybari, B., Darzi, M., Shafee, A., Li, Z. and Nguyen, T.K. (2019) Application of Nano-Refrigerant for Boiling Heat Transfer

Enhancement Employing an Experimental Study. *International Journal of Heat and Mass Transfer*, **141**, 974-980. https://doi.org/10.1016/j.ijheatmasstransfer.2019.07.043

[7] Abu-Nada, E. (2009) Effects of Variable Viscosity and Thermal Conductivity of Al_2O_3-Water Nanofluid on Heat Transfer Enhancement in Natural Convection. *International Journal of Heat and Fluid Flow*, **30**, 679-690. https://doi.org/10.1016/j.ijheatfluidflow.2009.02.003

[8] Huminic, G. and Huminic, A. (2018) Hybrid Nanofluids for Heat Transfer Applications—A State-of-the-Art Review. *International Journal of Heat and Mass Transfer*, **125**, 82-103. https://doi.org/10.1016/j.ijheatmasstransfer.2018.04.059

[9] Hussein, A.M., Bakar, R.A., Kadirgama, K. and Sharma, K.V. (2014) Heat Transfer Enhancement Using Nanofluids in an Automotive Cooling System. *International Communications in Heat and Mass Transfer*, **53**, 195-202. https://doi.org/10.1016/j.icheatmasstransfer.2014.01.003

[10] Sidik, N.A.C., Adamu, I.M., Jamil, M.M., Kefayati, G.H.R., Mamat, R. and Najafi, G. (2016) Recent Progress on Hybrid Nanofluids in Heat Transfer Applications: A Comprehensive Review. *International Communications in Heat and Mass Transfer*, **78**, 68-79. https://doi.org/10.1016/j.icheatmasstransfer.2016.08.019

[11] Ibrahim, N.I., Al-Sulaiman, F.A., Rahman, S., Yilbas, B.S. and Sahin, A.Z. (2017) Heat Transfer Enhancement of Phase Change Materials for Thermal Energy Storage Applications: A Critical Review. *Renewable and Sustainable Energy Reviews*, **74**, 26-50. https://doi.org/10.1016/j.rser.2017.01.169

[12] Swallom, D.W., Sadovnik, I., Gibbs, J.S., Gurol, H., Nguyen, L.V. and Van Den Bergh, H.H. (1991) Magnetohydrodynamic Submarine Propulsion Systems. *Naval Engineers Journal*, **103**, 141-157. https://doi.org/10.1111/j.1559-3584.1991.tb00945.x

[13] Chen, X., Ye, H., Zhao, L., Peng, A. and Wang, F. (2021) Thrust Distribution Characteristics and Structural Strength Analysis of the MHD Propeller with a Helical Channel. *Magnetohydrodynamics*, **57**, 17-26.

[14] Khan, M.A. and Kosel, J. (2021) Integrated Magnetohydrodynamic Pump with Magnetic Composite Substrate and Laser-Induced Graphene Electrodes. *Polymers*, **13**, Article 1113. https://doi.org/10.3390/polym13071113

[15] Waqas, H., Naeem, H., Manzoor, U., Sivasankaran, S., Alharbi, A.A., Alshomrani, A.S. and Muhammad, T. (2022) Impact of Electro-Magneto-Hydrodynamics in Radiative Flow of Nanofluids between Two Rotating Plates. *Alexandria Engineering Journal*, **61**, 10307-10317. https://doi.org/10.1016/j.aej.2022.03.059

[16] Haq, R.U., Hammouch, Z. and Khan, W.A. (2016) Water-Based Squeezing Flow in the Presence of Carbon Nanotubes between Two Parallel Disks. *Thermal Science*, **20**, 1973-1981. https://doi.org/10.2298/TSCI141102148H